Water−Hydroxide Exchange Reactions at the Catalytic Site of Heme−Copper Oxidases

Magnus Brändén,[‡] Andreas Namslauer,[‡] Örjan Hansson,[§] Roland Aasa,[||] and Peter Brzezinski*[,‡]

Department of Biochemistry and Biophysics, The Arrhenius Laboratories for Natural Sciences, Stockholm University, SE-106 91 Stockholm, Sweden, Department of Biochemistry and Biophysics, Göteborg University, P.O. Box 462, SE-405 30 Göteborg, Sweden, and Department of Chemistry and Bioscience, Chalmers University of Technology, P.O. Box 462, SE-405 30 Göteborg, Sweden

Received May 7, 2003; Revised Manuscript Received September 11, 2003

ABSTRACT: Membrane-bound heme−copper oxidases catalyze the reduction of O_2 to water. Part of the free energy associated with this process is used to pump protons across the membrane. The O_2 reduction reaction results in formation of high-pK_a protonatable groups at the catalytic site. The free energy associated with protonation of these groups is used for proton pumping. One of these protonatable groups is OH^-, coordinated to the heme and Cu_B at the catalytic site. Here we present results from EPR experiments on the *Rhodobacter sphaeroides* cytochrome *c* oxidase, which show that at high pH (9) ∼50% of oxidized heme a_3 is hydroxide-ligated, while at low pH (6.5), no hydroxide is bound to heme a_3. The kinetics of hydroxide binding to heme a_3 were investigated after dissociation of CO from heme a_3 in the enzyme in which the heme a_3−Cu_B center was reduced while the remaining redox sites were oxidized. The dissociation of CO results in a decrease of the midpoint potential of heme a_3, which results in electron transfer ($\tau \cong 3\ \mu$s) from heme a_3 to heme *a* in ∼100% of the enzyme population. At pH >7.5, the electron transfer is followed by proton release from a H_2O molecule to the bulk solution ($\tau \cong 2$ ms at pH 9). This reaction is also associated with absorbance changes of heme a_3, which on the basis of the results from the EPR experiments are attributed to formation of hydroxide-ligated heme a_3. The OH^- bound to heme a_3 under equilibrium conditions at high pH is also formed transiently after O_2 reduction at low pH. It is proposed that the free energy associated with electron transfer to the binuclear center and protonation of this OH^- upon reduction of the recently oxidized enzyme provides the driving force for the pumping of one proton.

Cytochrome *c* oxidase is an integral membrane protein complex, which catalyzes the reduction of O_2 to H_2O using cytochrome *c* as an electron donor. The protein scaffold holds four redox-active metal sites, Cu_A,[1] heme *a*, and the heme a_3−Cu_B binuclear center, which is the catalytic site of the enzyme. In the oxidases investigated to date, the substrate protons, used for reduction of O_2 to water, are taken up from the negative (*N*) side of the membrane and are transferred from the bulk solution to the binuclear center, consisting of heme a_3 and Cu_B, located within the membrane-spanning part of the enzyme. In addition, part of the energy released in the redox reaction is conserved by vectorial transfer of protons from the *N*-side to the positive (*P*) side across the membrane, thereby maintaining an electrochemical proton gradient that is used for synthesis of ATP (for reviews, see refs *1* and *2*). Two proton transfer pathways leading from the *N*-side surface toward the binuclear center have been identified (*3*−*5*). In cytochrome *c* oxidase from *Rhodobacter sphaeroides*, one of the pathways (D-pathway) starts with Asp(I-132)[2] and leads to Glu(I-286) from where protons can be transferred either toward the binuclear center or toward the output side of the enzyme. The other pathway (K-pathway) starts at the *N*-side surface at Glu(II-101) and leads via a highly conserved Lys(I-362) and Thr(I-359) to the binuclear center (Figure 1).

During reduction of the binuclear center, two protons are taken up to compensate for the negative charge introduced into the catalytic site (*6*), at least one of which is taken up through the K-pathway. When O_2 binds to the reduced binuclear center, the oxygen−oxygen bond is cleaved, forming an intermediate called **P**. In this state, a ferryl intermediate is formed at heme a_3 ($a_3^{4+}{=}O^{2-}$) and a hydroxide is bound to Cu_B ($Cu_B^{2+}{-}OH^-$). Four electrons and one proton are needed to break the oxygen−oxygen bond. Three of the electrons are supplied by the binuclear center ($a_3^{2+} \rightarrow a_3^{4+}$ and $Cu_B^{+} \rightarrow Cu_B^{2+}$), and the proton that is needed is presumably transferred from Tyr(I-288) (*7*). If the enzyme is initially fully reduced, the "fourth" electron is transferred from heme *a* (state $\mathbf{P_R}$). During formation of the next intermediate, **F**, a proton is transferred to the catalytic site through the D-pathway (*8*). It has been proposed

* To whom correspondence should be addressed. Fax: (+46)-8-153679. Phone: (+46)-8-163280. E-mail: peterb@dbb.su.se.

[‡] Stockholm University.

[§] Göteborg University.

[||] Chalmers University of Technology.

[1] Abbreviations: Cu_A, copper A; Cu_B, copper B; binuclear center, Cu_B and heme a_3; **O**, fully oxidized enzyme; $\mathbf{O}^{\sim}$, high-energy form of the oxidized enzyme; **E**, enzyme in which only Cu_B is reduced; $\mathbf{E}^{\sim}$, high-energy form of **E**; $\mathbf{P_R}$, peroxy intermediate (formed upon reaction of the fully reduced enzyme with O_2); **F**, oxo−ferryl intermediate; SD, standard deviation.

[2] If not otherwise indicated, amino acid residues are numbered according to the *R. sphaeroides* sequence.

10.1021/bi0347407 CCC: $25.00
Published on Web 10/21/2003

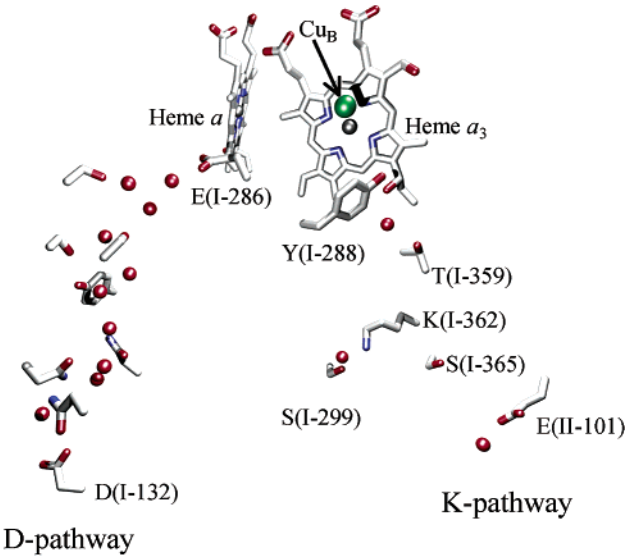

FIGURE 1: Structure of the proton transfer pathways, together with the heme groups and Cu_B (Cu_A not shown), in *R. sphaeroides* cytochrome *c* oxidase.

that the proton acceptor is the hydroxide bound to Cu_B, which is released as water (e.g., refs *9* and *10*). However, it is also possible that the proton is transferred to the unprotonated Tyr(I-288), which is supported by recent FTIR data (P. Rich, personal communication). This scenario would leave the OH^- bound to Cu_B in the **F** state. The transfer of the next electron to the catalytic site results in reduction of the ferryl intermediate and formation of a second hydroxide, bound to the oxidized heme a_3 (*11*). Since the oxidized enzyme has only one OH^- bound at the binuclear center, most likely to Cu_B (*4*, *12*), the heme a_3-bound OH^- is released (or protonated) after completion of the single-turnover reaction.

Two protons are pumped during the O_2 reduction reaction, coupled to the **P** to **F** and **F** to **O** transitions (*13*). Recently, it has also been shown that the reductive part of the reaction cycle (i.e., during reduction of the oxidized enzyme) is coupled to proton pumping. However, this only occurs upon re-reduction of the recently oxidized enzyme (*13*; see also ref *14*). An important question is why pumping only occurs on re-reduction and how the free energy from the preceding O_2 reduction is temporarily conserved by the enzyme.

The kinetics of proton uptake and release in the absence of O_2, coupled to internal electron transfer within the enzyme, can be investigated directly after flash photolysis of CO from the mixed-valence state (two-electron-reduced enzyme). In this state, heme *a* and Cu_A are oxidized and heme a_3 and Cu_B are reduced with CO bound to heme a_3 (*15*−*17*). The CO ligand stabilizes the reduced state of the binuclear center. Flash photolysis of CO from the mixed-valence enzyme results in internal electron transfer from heme a_3 to heme *a*, which in the enzyme from *R. sphaeroides* displays a time constant of ∼3 μs (refs *18* and *19* and this work). This electron transfer leaves the heme a_3 site oxidized and is followed by proton release on a millisecond time scale ($\tau \cong$ 2 ms at pH 9) to the bulk solution through the K-pathway (*20*, *21*; see also ref *22*). In the D-pathway mutant enzymes [e.g., EQ(I-286)] neither the rate nor the extent of proton release was affected (*8*). Concomitant with the proton release is an absorbance change, which has previously been attributed to additional electron transfer from heme a_3 to heme *a* coupled to the proton release (*23*). The amplitude of this absorbance change was shown to be pH-dependent, and the time constant of the kinetic phase decreases with an increase in pH (in the pH range of 7−11).

The properties of the metal centers in cytochrome *c* oxidase have been characterized extensively using EPR spectroscopy. When the binuclear center is oxidized, heme a_3 and Cu_B are magnetically coupled and do not give rise to any detectable EPR signals. If, however, Cu_B is reduced, heme a_3 becomes magnetically uncoupled from Cu_B, which makes it possible to detect signals originating from heme a_3 (*24*). Earlier studies have shown that the dissociation of the CO ligand from the mixed-valence enzyme results in a significant decrease in the magnitude of the $g = 3$ signal, due to the reduction of heme *a* (*25*). At the same time, an increase in the magnitude of the $g = 6$ signal is observed due to oxidation of heme a_3. In this study, we have extended the experiments to include measurements at high pH (8.9). The results show that at high pH, but not at low pH (6.5), a $g = 2.6$ signal is observed, previously attributed to a hydroxide-ligated low-spin heme a_3 (*26*). On the basis of these results, we re-interpret the origin of the absorbance difference spectrum of the millisecond absorbance changes at high pH, discussed above to be associated with formation of hydroxide-ligated heme a_3, i.e., the transition of heme a_3 from a high-spin to a low-spin state. An OH^- is also bound transiently to heme a_3 at low pH upon oxidation of the reduced enzyme in the normal reaction cycle. We propose that the free energy associated with re-reduction of heme a_3 and protonation of this OH^- may be used for proton pumping.

MATERIALS AND METHODS

Purification of Cytochrome c Oxidase. The *R. sphaeroides* bacteria were grown aerobically in shake incubators at 30 °C. The cells were harvested, and the enzyme was purified as described previously (*27*). After elution from the Ni^{2+} column, the buffer was exchanged with 0.1 M Hepes-KOH (pH 7.4) and 0.1% dodecyl β-D-maltoside. The enzyme was frozen in liquid nitrogen and stored in a −80 °C freezer until it was used. The enzyme from bovine heart was prepared as described previously (*28*).

Preparation of the Mixed-Valence CO-Bound Complex. The buffer was exchanged with 0.1 M CHES (pH 9) [or 0.1 M HEPES (pH 7)] and 0.1% dodecyl β-D-maltoside. In experiments with the bovine heart enzyme, 130 mM KCl was added to the buffer at pH 7. Before proton release to the bulk solution was measured, the buffer was exchanged with 0.1 M KCl. The enzyme solution, at a concentration of ∼5 μM, was transferred to a sealed cuvette, and the atmosphere was exchanged first with nitrogen and then with carbon monoxide. Carbon monoxide, which is a two-electron donor, reduces the enzyme to yield the mixed-valence CO-bound state (*29*). Initially, the two-electron-reduced form (mixed-valence state) of the enzyme was formed, as characterized by its optical absorption spectrum. However, prolonged incubation in CO at high pH resulted also in reduction of the heme *a*−Cu_A center in a small fraction of the enzyme population. When this additional reduction was observed, the sample was titrated with ferricyanide until an absorption spectrum characteristic of a pure two-electron

mixed-valence state was obtained. The enzyme concentration with CO bound was determined in the kinetic experiments from the CO dissociation absorbance changes at 445 nm.

Flash Photolysis of CO from the Mixed-Valence State of the Enzyme. A 5 ns laser pulse (Brilliant B from Quantel) was used to dissociate CO from the reduced heme a_3. Time-resolved optical absorption spectroscopy (setup purchased from Applied Photophysics, LKS.60) was used to monitor the absorbance changes following the dissociation of CO. Monochromators both in front of and behind the cuvette were used to select the appropriate wavelength. The proton release associated with oxidation of heme a_3 was measured using the pH-sensitive dye, cresol purple, at 560 nm. The difference in absorbance between an unbuffered and buffered solution was measured to exclude any contribution in absorbance from the hemes, and the response of the dye was calibrated by titration with 2 mM HCl.

Deconvolution of Heme a and Heme a_3 Redox Difference Spectra. A sample of oxidized cytochrome *c* oxidase (3 mL, 3 μM), in 100 mM HEPES (pH 7.4), was divided equally in two anaerobic cuvettes after which the atmosphere was exchanged with N_2 by flushing wet gas (i.e., bubbled through water so that the enzyme concentration did not change) over the surface and carefully shaking the cuvette several times. The optical spectrum was then recorded (called spectrum I).

Cuvette 1. The enzyme was reduced with ascorbate using PMS as a redox mediator (spectrum II). The atmosphere was then exchanged with CO, as described above (spectrum IV).

Cuvette 2. The atmosphere was exchanged with CO which is a two-electron reductant. The oxidized enzyme then becomes reduced to yield the CO-bound mixed-valence state, having the heme a_3-Cu_B center reduced and heme a/Cu_A oxidized (spectrum III). To verify that 100% of the CO-bound mixed-valence state was formed, the absorbance change at 445 nm, upon photodissociation of CO, was compared to that observed with the fully reduced enzyme. The mixed-valence enzyme was then reduced with ascorbate using PMS as a redox mediator to yield the CO-bound fully reduced state (spectrum IV).

The difference spectra were derived from the optical absorption spectra described above (assuming a negligible contribution from Cu_A in the visible range of the spectrum): (I) spectrum of the fully oxidized enzyme, (II) spectrum of the fully reduced enzyme, (III) spectrum of the CO-bound mixed-valence enzyme, and (IV) spectrum of the CO-bound fully reduced enzyme. Heme $a_{(red-ox)}$ = IV − III, which yields the static difference spectrum of reduced minus oxidized heme *a*. Heme $a_{3(red-ox)}$ = (II − I) − (IV − III), which yields the static difference spectrum of reduced minus oxidized heme a_3.

Preparation of EPR Samples. The buffer was exchanged with 0.1 M CHES (pH 8.9) or 0.1 M MES (pH 6.5), each supplemented with 0.1% dodecyl β-D-maltoside. The enzyme was concentrated to ~100 μM using CentriPrep concentration columns and transferred to EPR tubes, which were sealed. The atmosphere was then exchanged as described above to yield the mixed-valence CO-bound state. Carbon monoxide was dissociated from the reduced heme a_3 using a strong white light (xenon lamp, 150 W). The optical absorption spectrum of the enzyme was recorded both before and under illumination using a spectrophotometer (Cary 50) to ensure that CO had dissociated. The sample in the EPR tube was then, under continuous illumination, frozen in liquid nitrogen. Illumination of the enzyme with strong white light leads to reduction of the enzyme with more than two electrons in a fraction of the enzyme population. The sample in the EPR tube was therefore a mixture of the two- and three-electron-reduced enzyme. Ferricyanide was not added to yield the two-electron-reduced state because of its interference with the EPR spectrum of the enzyme.

EPR Measurements. The EPR spectra were recorded with a Bruker ESP 380 E X-band spectrometer equipped with a standard TE102 rectangular cavity and an Oxford Instruments ESR-900 helium-flow cryostat. Experimental conditions were as follows: temperature, 10 K; microwave power, 0.02 mW; microwave frequency, 9.47 GHz; modulation amplitude, 2 mT; and time constant, 164 ms. Integration of EPR signals was performed as described in ref *30*.

RESULTS

Carbon monoxide reduces the oxidized cytochrome *c* oxidase, forming the mixed-valence state of the enzyme, in which the binuclear center is reduced and heme *a* and Cu_A are oxidized. The bound CO stabilizes the reduced state of heme a_3. As shown previously, flash photolysis of the CO ligand results in a decrease of the apparent midpoint potential of heme a_3, which results in electron equilibration between the hemes with a time constant of ~3 μs (termed the "microsecond phase") (*18*, *19*). The other redox site in the binuclear center, Cu_B, remains reduced upon dissociation and recombination of CO to heme a_3. In a small fraction (≤5%) of the enzyme population, an electron is also transferred to Cu_A with a time constant of ~30 μs.

At high pH (>7.5), the rapid electron transfer between the hemes is followed by an absorbance change and a net proton release to the bulk solution on a millisecond time scale (termed the "millisecond phase") (*15*−*17*).

Microsecond Phase. Figure 2A shows absorbance changes at 445 nm after flash photolysis of CO from the mixed-valence *R. sphaeroides* and bovine heart enzymes. After the initial increase in absorbance, associated with dissociation of CO, there is a decrease in absorbance due to electron transfer from heme a_3 to heme *a*. The different amplitudes of this phase in the two kinetic traces are due to the different extents of electron transfer in the two enzymes (see below). Figure 2B shows the kinetic difference spectra[3] of the microsecond phase in the *R. sphaeroides* and bovine heart (*19*) enzymes. The amplitudes of the kinetic difference spectra correspond to electron transfer from heme a_3 to heme *a* in ~100 and ~30%[4] of the enzyme populations in the *R. sphaeroides* and bovine heart enzymes, respectively. The figure also shows the static difference spectrum of the latter enzyme corresponding to equimolar oxidation of heme a_3 and reduction of heme *a* [double-difference spectrum of heme $a_{(red-ox)}$ − heme $a_{3(red-ox)}$; see Materials and Methods].

Millisecond Phase. Figure 3A shows absorbance changes on a millisecond time scale at 598 nm. The increase in absorbance ($\tau \cong 2$ and 5 ms at pH 9 for the *R. sphaeroides*

[3] A kinetic difference spectrum is defined as the difference in absorbance of a kinetic phase measured at infinite and zero times.

[4] It is difficult to estimate the error because of, for example, spectral interactions between the hemes.

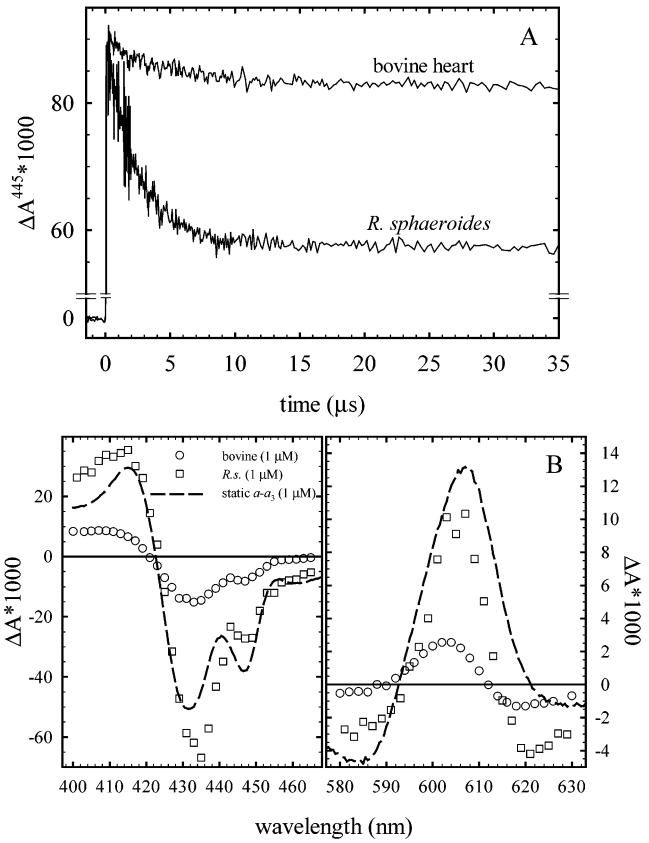

FIGURE 2: (A) Absorbance changes at 445 nm following dissociation of CO from the mixed-valence bovine heart and *R. sphaeroides* enzymes. (B) Kinetic difference spectra of the 3 μs phase observed after photolysis of CO from the mixed-valence bovine heart (○) and *R. sphaeroides* (*R.s.*) (□) enzymes and static double-difference spectrum of heme $a_{(\text{red}-\text{ox})}$ − heme $a_{3(\text{red}-\text{ox})}$ (− − −) (see Materials and Methods). Experimental conditions were as follows: 5 μM cytochrome *c* oxidase in 0.1% dodecyl β-D-maltoside, 100 mM HEPES (pH 7), and 1 mM CO at 20 °C. In the bovine enzyme sample, 130 mM KCl was included. All traces are scaled to 1 μM reacting enzyme (see Materials and Methods).

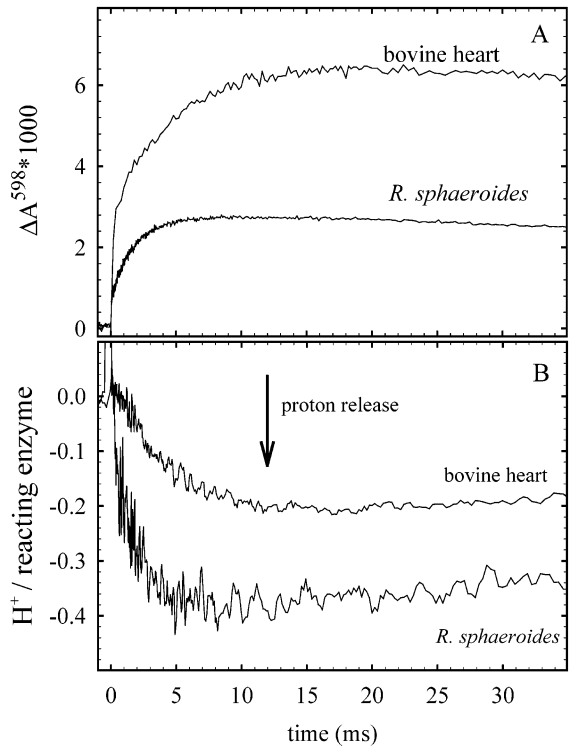

FIGURE 3: Absorbance changes of the heme groups at 598 nm (millisecond phase) (A) and the dye cresol purple at 560 nm (B) following dissociation of CO from the mixed-valence bovine heart and *R. sphaeroides* enzymes (as indicated). In panel B, the traces are the differences of traces obtained in buffer-free and buffered solutions. Experimental conditions were as follows: 5 μM cytochrome *c* oxidase in 0.1% dodecyl β-D-maltoside, 100 mM KCl (for the buffer-free solution in panel B), 100 mM CHES (pH 9) (in panel A and buffered solution in panel B), 40 μM cresol purple (in panel B), and 1 mM CO at 20 °C. All traces are scaled to 1 μM reacting enzyme.

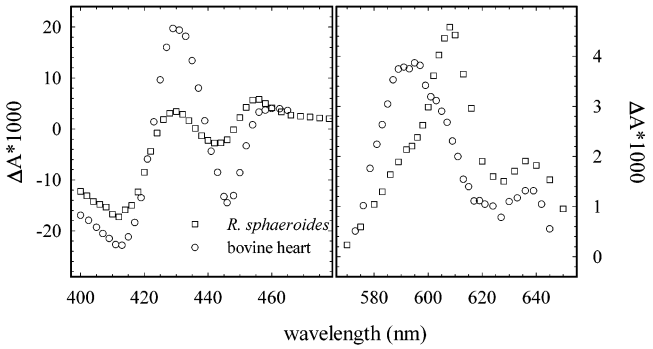

FIGURE 4: Kinetic difference spectra of the millisecond phase ($\tau \cong 5$ and 2 ms) measured after photolysis of CO from the mixed-valence bovine heart (○) and *R. sphaeroides* (□) enzymes. Experimental conditions were the same as those for Figure 3A. All traces are scaled to 1 μM reacting enzyme.

and bovine heart enzymes, respectively) has previously been attributed to electron transfer from heme a_3 to heme *a*, coupled to proton release to the bulk solution (*23*). As shown in Figure 3B, the number of protons released per reacting enzyme in the *R. sphaeroides* and bovine heart enzymes at pH 9 is 0.4 ± 0.1 (SD, $n = 3$) and 0.2 ± 0.05 (SD, $n = 6$), respectively. When the fractions of electron transfer from heme a_3 to heme *a* in these two enzymes are taken into account (see above), the number of protons released per transferred electron is ∼0.4 and ∼0.7 in the *R. sphaeroides* and bovine heart enzymes, respectively.

We monitored the absorbance changes on the millisecond time scale after the dissociation of CO at a large number of wavelengths in both the Soret and α regions (Figure 4). As seen in Figure 4, the kinetic difference spectrum of the millisecond phase is different from that of the microsecond phase (cf. Figure 2B). Hence, the kinetic phase cannot be attributed to a pure electron transfer from heme a_3 to heme *a*.

EPR Spectra of the CO-Dissociated State. The use of the EPR technique has the advantage of distinguishing the redox and spin states of heme *a* and heme a_3, respectively. An EPR spectrum was recorded of the equilibrium state that is reached after CO has been permanently dissociated from the mixed-valence state of the enzyme by means of continuous illumination. Because the white light that is used to dissociate CO induces further reduction, heme *a* and Cu_A also become reduced in a small fraction of the enzyme population. Even though the CO-dissociated three- and two-electron-reduced states have different distributions of the electrons between the metal centers, information is still obtained about the relative fractions of the low- and high-spin states of heme a_3 in the enzyme fraction in which heme a_3 is oxidized. As shown in Figure 5, only at high pH (8.9) but not at low pH

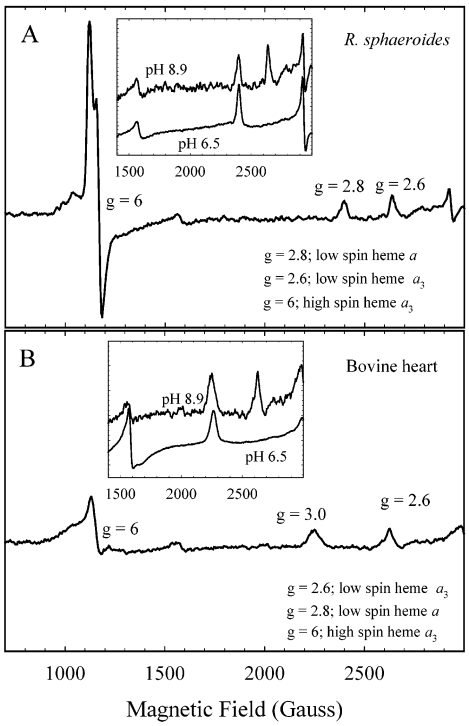

FIGURE 5: EPR spectra at 10 K obtained after photolysis of CO from the mixed-valence cytochrome *c* oxidase from *R. sphaeroides* (A) (concentration of 82 μM) and bovine heart (B) (concentration of 135 μM) at pH 8.9. The inset shows a comparison of the low-spin heme spectral region at pH 8.9 and 6.5. See Materials and Methods for spectrometer settings. The buffers contained 0.1% dodecyl β-D-maltoside, 1 mM CO, and 100 mM CAPS at pH 9 or 100 mM MES at pH 6.5, at a temperature of 10 K.

(6.5) is the $g = 2.6$ signal, originating from low-spin heme a_3, present. Hence, at pH 6.5, heme a_3 is exclusively in a high-spin state, while at pH 8.9, the low-spin form corresponds to 40 and 50% of the fraction of enzyme molecules in which heme a_3 is oxidized (i.e., not of the entire enzyme population) in the *R. sphaeroides* and bovine heart enzymes, respectively. It should also be noted that the fraction of oxidized heme a_3 during the 3 μs electron transfer is smaller in the bovine than in the *R. sphaeroides* enzyme (cf. Figure 3A).

The low-spin signal is split into two peaks in both enzymes with *g* values of 2.60 and 2.56 (*R. sphaeroides*) and 2.62 and 2.57 (bovine heart), respectively, and both peaks were included in the integration. Since the high-field peak saturates more easily than the low-field peak and contributes approximately two-thirds to the total signal, spectra were acquired at a sufficiently low microwave power to ensure a full development of the signals.

DISCUSSION

Microsecond Phase. As shown previously for the bovine enzyme (*19*) also with the *R. sphaeroides* enzyme, the kinetic difference spectrum of the 3 μs phase fits relatively well with the static absorbance difference spectrum corresponding to an electron transfer from heme a_3 to heme *a* (Figure 2B). The deviation may be due to, for example, spectral interactions between the heme groups (different redox states in the static and kinetic experiments) or the coordination of water in the enzyme with oxidized heme a_3, used to record the static spectrum, but not in the kinetic experiment.

The different extents of electron transfer in the microsecond phase in the bovine heart and *R. sphaeroides* enzymes show that the equilibrium constants between the hemes are different in the two enzymes (*18*). The extent of electron transfer in the *R. sphaeroides* enzyme differs from that reported previously in our laboratory (*18*). This is because in the previous study the extent of electron transfer was determined from measurements at a single wavelength (445 nm), and in addition, it was underestimated due to a poorer time resolution of the measuring system.

After electron transfer to heme *a*, there is also a slower equilibration, with a time constant of ~30 μs, with Cu_A. In the mixed-valence enzyme, this electron transfer takes place in a negligible fraction (~5%) of the enzyme population. In the EPR samples, in which a fraction of the enzyme population is in the three-electron-reduced state, the equilibrium between heme *a* and Cu_A is more shifted toward Cu_A. However, since in these experiments only the relative populations of the low- and high-spin forms of oxidized heme a_3 are considered, the results are independent of the population of reduced Cu_A.

Millisecond Phase. At high pH (>7.5), the 3 μs electron transfer from heme a_3 to heme *a* is followed by proton release to the bulk solution through the K-pathway. Several different possible proton donors were suggested for release of the proton, where one likely candidate is a water molecule that releases a proton, followed by hydroxide binding to the oxidized heme a_3 (*17*, *20*). On the basis of the pH dependence of the rate and extent of the reaction, a pK_a of ~9 (*17*, *18*) was estimated for the protonatable group from which the proton is released. In the previous studies using the bovine heart enzyme, the spectral changes associated with the millisecond phase were interpreted in terms of electron transfer from heme a_3 to heme *a*. This cannot be the case for the *R. sphaeroides* enzyme because in this enzyme heme a_3 becomes essentially fully oxidized during the 3 μs phase. In addition, as seen in Figure 4, the kinetic difference spectra of the millisecond phase in both the bovine heart and *R. sphaeroides* enzymes are distinctly different from the double-difference spectrum of heme $a_{(red-ox)}$ − heme $a_{3(red-ox)}$. However, in the bovine heart enzyme, in which electron transfer occurs in ~30% of the enzyme population, the proton release upon oxidation of heme a_3 is likely to shift the electron equilibrium between the hemes, resulting in additional electron transfer to heme *a* on the millisecond time scale. In fact, a possible explanation for the different shapes of the kinetic difference spectra of the millisecond phase obtained with the *R. sphaeroides* and bovine heart enzymes is likely to be the additional electron transfer in the bovine enzyme.

The kinetic difference spectrum of the millisecond phase (Figure 4) shows that the result of the reaction is a shift of the Soret band peaks. A shift of the Soret band by ~5 nm was observed with myoglobin and hemoglobin upon replacement of H_2O with OH^- at the heme (summarized in ref *31*). It is difficult to quantify the shift observed in cytochrome *c* oxidase because it is difficult to assess whether there is time for H_2O to bind to the oxidized heme a_3 after CO dissociation (and the 3 μs electron transfer from heme a_3 to heme *a*), prior to formation of hydroxide-ligated heme a_3 (see also below).

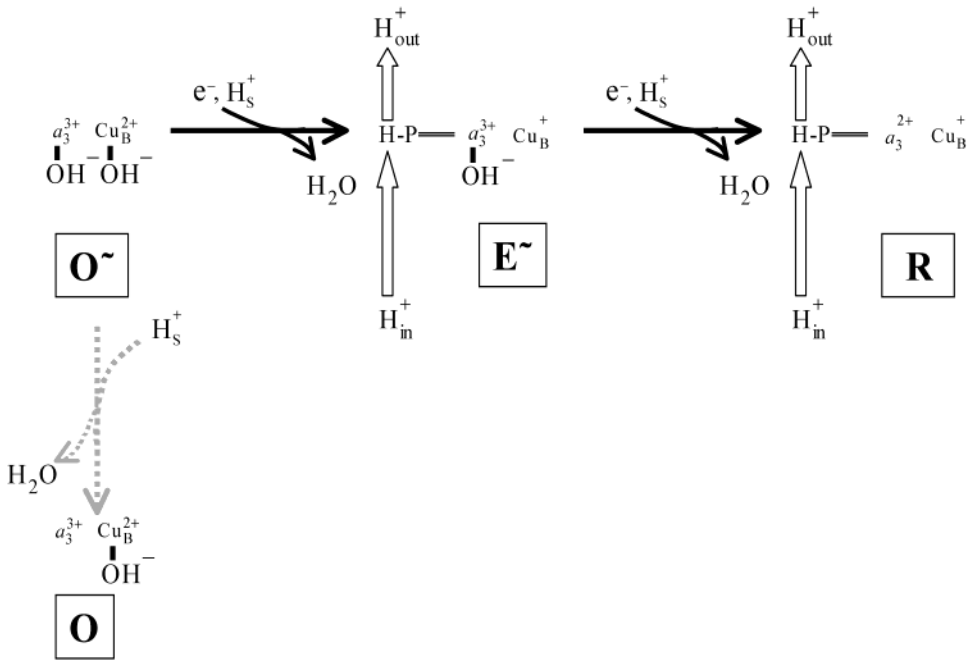

FIGURE 6: Model illustrating the events at the binuclear center upon re-reduction of the recently oxidized (see the text) cytochrome *c* oxidase (based on the experimental results from this study). The superscript ~ indicates a high-energy state (*13*). If not reduced, the $\mathbf{O}^{\sim}$ state relaxes spontaneously to the **O** state in which there is an OH^- bound only to Cu_B. If not further reduced, the $\mathbf{E}^{\sim}$ state relaxes to the **E** state in which heme a_3 is oxidized and Cu_B is reduced with no ligands bound at the binuclear center. Proton pumping (via the "pump site", P) is suggested to take place upon reduction of states in which there is a hydroxide bound to heme a_3. H_S^+ represents "substrate protons" used during reduction of O_2 to H_2O.

EPR Experiments. In an earlier study (*26*), cytochrome *c* oxidase from bovine heart was titrated with ferrocytochrome *c* at pH 6.4, 7.4, and 8.4. At pH 6.4, only the high-spin form of heme a_3 ($g = 6$) was present, while at pH 8.4, in 50−70% of the enzyme population the high-spin form was converted to a low-spin form ($g = 2.6$). It was proposed that the transition from high to low spin represents a change in the sixth ligand of heme a_3 from H_2O to OH^-, as had previously been observed with other proteins, such as ferrimyoglobin (*31*). To determine the spin state of the oxidized heme a_3 after dissociation of CO from the mixed-valence enzyme, we recorded the EPR spectrum of the equilibrium state that is obtained when CO is permanently dissociated from heme a_3. This state is the same as that formed after the millisecond phase in the kinetic experiments. In both the *R. sphaeroides* and bovine enzymes at pH 6.5, the oxidized heme a_3 displayed exclusively the high-spin state. With an increase in pH to 8.9, in the *R. sphaeroides* and bovine enzymes, ~40 and ~50%, respectively, of the oxidized heme a_3 was found in a low-spin, ligand-bound state. Thus, the pK_a of this transition is ~9, consistent with that determined previously from the pH dependence of the rate and extent of the millisecond phase (see above). We note that the extent of proton release after dissociation of CO is approximately the same as the fraction of the low-spin state, which is consistent with the fraction of hydroxide formed at the oxidized heme a_3. However, the comparison of the extents of proton release and the hydroxide formed at heme a_3 can only be made qualitatively, since the EPR measurements were taken at cryogenic temperatures, at which the pK_a of the water molecule is likely to be different from that at room temperature.

The $g = 6$ signal originating from the high-spin heme a_3 consists of both an axial and a rhombic component. Axial and rhombic $g = 6$ signals are sometimes attributed to six- and five-coordinated heme, respectively, although this is not entirely unambiguous (see ref *32* and references therein). The axial contribution could thus be due to a water molecule that is bound to heme a_3 in a fraction of the enzyme. However, this situation may apply only to the EPR experiments since these measurements were done under steady-state conditions where there is sufficient time for water to bind after dissociation of CO.

Functional Significance of the OH^- Bound to Heme a_3. On the basis of the discussion above, we conclude that in ~50% of the enzyme population at pH 8.9, on the time scale of the millisecond phase, a water molecule (which may be bound to heme a_3; see above) at the catalytic site releases a proton followed by hydroxide formation at the oxidized heme a_3. Results from recent studies have shown that contrary to what was previously believed, not only the oxidative but also the reductive part of the reaction cycle of cytochrome *c* oxidase is associated with proton pumping. However, the reduction of the binuclear center is only coupled to proton translocation if the enzyme is re-reduced immediately after it has been recently oxidized (*13*). The state formed immediately after oxidation was denoted $\mathbf{O}^{\sim}$, which is a "high-energy state" of the oxidized enzyme in which the free energy needed for proton translocation is stored within the protein structure. If the enzyme is not re-reduced within a short time, it relaxes to the oxidized state, **O**. The difference in the structures of **O** and $\mathbf{O}^{\sim}$ is unknown. On the basis of the results presented in this study, we can now suggest one possible structural origin of the $\mathbf{O}^{\sim}$ state.

As described in the introductory section, two hydroxides are likely to be formed at the binuclear center in the last step of O_2 reduction (see also ref *11*). This state, which in the reaction of the fully reduced enzyme with O_2 is formed

with a time constant of ~1 ms (at pH 7), is not in equilibrium with the surrounding solution at pH 7, and therefore, the heme a_3-bound hydroxide becomes protonated and released as water. Indeed, an electrogenic reaction with a time constant of ~5 ms has been observed (*33*, *34*), and we previously observed that after oxidation of the enzyme, there is a slower proton uptake with a time constant of 5−10 ms. This proton uptake reaction was not observed with the K-pathway mutant enzymes, which indicates that the proton uptake takes place through the K-pathway (*16*, *20*). We propose that the initially formed oxidized state with two hydroxide molecules bound at the binuclear center is a "high-energy state" $\mathbf{O}^{\sim}$ (Figure 6), which, if not immediately reduced, relaxes spontaneously to **O** with one OH^- bound only to Cu_B, accompanied by proton uptake through the K-pathway. The injection of one electron into the enzyme in state $\mathbf{O}^{\sim}$ results in reduction of Cu_B and protonation of the Cu_B-bound hydroxide. The state that is formed is the same as that investigated in this study, i.e., with Cu_B reduced and an OH^- bound to the oxidized heme a_3. This state is called $\mathbf{E}^{\sim}$. It is an unstable state, which at pH 7 would relax spontaneously to the one-electron-reduced binuclear (Cu_B) center, denoted **E**, which is accompanied by exergonic protonation of the hydroxide. The results from this study indicate that the pK_a of the heme a_3-bound hydroxide is ~9. Thus, if only the hydroxide bound at heme a_3 is considered, at pH 7 the free energy difference between the $\mathbf{E}^{\sim}$ state and the relaxed **E** state is ~120 meV (corresponding to protonation of a group with a pK_a of 9 at pH 7).

In the oxidized enzyme, the reduction of Cu_B and heme a_3 by two molecules of cytochrome *c* is associated with a change in free energy of approximately −250 meV (see refs *1* and *24*). Since the electron transfer to the binuclear center is associated with the protonation of the two hydroxides bound to heme a_3 and Cu_B, the overall driving force provided by both reactions may be used for proton translocation. It is, however, difficult to estimate the driving force for the protonation of the first hydroxide in state $\mathbf{O}^{\sim}$ (see Figure 6; cf. discussion above on the driving force for the protonation of the second hydroxide). The model is consistent with results from studies of the pH dependence of proton pumping in *Escherichia coli* cytochrome bo_3, which show that the proton pumping stoichiometry decreases with an increase in pH (*35*).

In conclusion, the results from this work show that a hydroxide with a pK_a of ~9 is bound to oxidized heme a_3 when Cu_B is reduced. A hydroxide bound to oxidized heme a_3 is also formed transiently immediately after O_2 reduction. We suggest that the free energy available from protonation of this hydroxide can be made available for proton translocation if the enzyme becomes reduced before the hydroxide is released.

ACKNOWLEDGMENT

We thank Tore Vänngård for helpful discussions and critical reading of the manuscript and Ida Holmgren for technical assistance.

REFERENCES

1. Babcock, G. T., and Wikström, M. (1992) *Nature 356*, 301−309.
2. Ferguson-Miller, S., and Babcock, G. T. (1996) *Chem. Rev. 96*, 2889−2907.
3. Iwata, S., Ostermeier, C., Ludwig, B., and Michel, H. (1995) *Nature 376*, 660−669.
4. Svensson-Ek, M., Abramson, J., Larsson, G., Törnroth, S., Brzezinski, P., and Iwata, S. (2002) *J. Mol. Biol. 321*, 329−339.
5. Tsukihara, T., Aoyama, H., Yamashita, E., Tomizaki, T., Yamaguchi, H., Shinzawa-Itoh, K., Nakashima, R., Yaono, R., and Yoshikawa, S. (1996) *Science 272*, 1136−1144.
6. Mitchell, R., and Rich, P. R. (1994) *Biochim. Biophys. Acta 1186*, 19−26.
7. Babcock, G. T. (1999) *Proc. Natl. Acad. Sci. U.S.A. 96*, 12971−12973.
8. Ädelroth, P., Svensson-Ek, M., Mitchell, D. M., Gennis, R. B., and Brzezinski, P. (1997) *Biochemistry 36*, 13824−13829.
9. Morgan, J. E., Verkhovsky, M. I., Palmer, G., and Wikström, M. (2001) *Biochemistry 40*, 6882−6892.
10. Zaslavsky, D., and Gennis, R. B. (2000) *Biochim. Biophys. Acta 1458*, 164−179.
11. Han, S., Ching, Y. C., and Rousseau, D. L. (1990) *Nature 348*, 89−90.
12. Fann, Y. C., Ahmed, I., Blackburn, N. J., Boswell, J. S., Verkhovskaya, M. L., Hoffman, B. M., and Wikström, M. (1995) *Biochemistry 34*, 10245−10255.
13. Verkhovsky, M. I., Jasaitis, A., Verkhovskaya, M. L., Morgan, J. E., and Wikström, M. (1999) *Nature 400*, 480−483.
14. Ruitenberg, M., Kannt, A., Bamberg, E., Fendler, K., and Michel, H. (2002) *Nature 417*, 99−102.
15. Ädelroth, P., Sigurdson, H., Hallén, S., and Brzezinski, P. (1996) *Proc. Natl. Acad. Sci. U.S.A. 93*, 12292−12297.
16. Brändén, M., Sigurdson, H., Namslauer, A., Gennis, R. B., Ädelroth, P., and Brzezinski, P. (2001) *Proc. Natl. Acad. Sci. U.S.A. 98*, 5013−5018.
17. Sigurdson, H., Brändén, M., Namslauer, A., and Brzezinski, P. (2002) *J. Inorg. Biochem. 88*, 335−342.
18. Ädelroth, P., Brzezinski, P., and Malmström, B. G. (1995) *Biochemistry 34*, 2844−2849.
19. Namslauer, A., Brändén, M., and Brzezinski, P. (2002) *Biochemistry 41*, 10369−10374.
20. Ädelroth, P., Gennis, R. B., and Brzezinski, P. (1998) *Biochemistry 37*, 2470−2476.
21. Brändén, M., Tomson, F., Gennis, R. B., and Brzezinski, P. (2002) *Biochemistry 41*, 10794−10798.
22. Kotelnikov, A. I., Medvedev, E. S., Medvedev, D. M., and Stuchebrukhov, A. A. (2001) *J. Phys. Chem. B 105*, 5789−5796.
23. Hallén, S., Brzezinski, P., and Malmström, B. G. (1994) *Biochemistry 33*, 1467−1472.
24. Wikström, M., Krab, K., and Saraste, M. (1981) *Cytochrome c oxidase*: *A synthesis*, Academic Press, San Diego.
25. Leigh, J. S., Jr., Wilson, D. F., Owen, C. S., and King, T. E. (1974) *Arch. Biochem. Biophys. 160*, 476−486.
26. Lanne, B., Malmström, B. G., and Vänngård, T. (1979) *Biochim. Biophys. Acta 545*, 205−214.
27. Mitchell, D. M., and Gennis, R. B. (1995) *FEBS Lett. 368*, 148−150.
28. Brandt, U., Schägger, H., and von Jagow, G. (1989) *Eur. J. Biochem. 182*, 705−711.
29. Brzezinski, P., and Malmström, B. G. (1985) *FEBS Lett. 187*, 111−114.
30. Aasa, R., Albracht, S. P. J., Falk, K.-E., Lanne, B., and Vänngård, T. (1976) *Biochim. Biophys. Acta 422*, 260−272.
31. Antonini, E., and Brunori, M. (1971) *Hemoglobin and myoglobin in their reactions with ligands*, Elsevier, Amsterdam.
32. Ikeda-Saito, M., Hori, H., Andersson, L. A., Prince, R. C., Pickering, I. J., George, G. N., Sanders, C. R., Lutz, R. S., McKelvey, E. J., and Mattera, R. (1992) *J. Biol. Chem. 267*, 22843−22852.
33. Zaslavsky, D., Kaulen, A. D., Smirnova, I. A., Vygodina, T., and Konstantinov, A. A. (1993) *FEBS Lett. 336*, 389−393.
34. Jasaitis, A., Verkhovsky, M. I., Morgan, J. E., Verkhovskaya, M. L., and Wikström, M. (1999) *Biochemistry 38*, 2697−2706.
35. Verkhovskaya, M., Verkhovsky, M., and Wikström, M. (1992) *J. Biol. Chem. 267*, 14559−14562.

BI0347407